

Coordinated control strategy for wind power accommodation based on electric heat storage and pumped storage

LI Shou-dong¹, DONG Hai-ying¹, ZHANG Rui-ping¹, MA Xi-ping²

(1. School of Automation and Electrical Engineering, Lanzhou Jiaotong University, Lanzhou 730070, China;

2. State Grid Gansu Electric Power Research Institute, Lanzhou 730050, China)

Abstract: To solve the severe problem of wind power curtailment in the winter heating period caused by “power determined by heat” operation constraint of cogeneration units, this paper analyzes thermoelectric load, wind power output distribution and fluctuation characteristics at different time scales, and finally proposes a two-level coordinated control strategy based on electric heat storage and pumped storage. The optimization target of the first-level coordinated control is the lowest operation cost and the largest wind power utilization rate. Based on prediction of thermoelectric load and wind power, the operation economy of the system and wind power accommodation level are improved with the cooperation of electric heat storage and pumped storage in regulation capacity. The second-level coordinated control stabilizes wind power real-time fluctuations by cooperating electric heat storage and pumped storage in control speed. The example results of actual wind farms in Jiuquan, Gansu verifies the feasibility and effectiveness of the proposed coordinated control strategy.

Key words: wind power accommodation; electric heat storage; pumped storage; wind power fluctuation; coordinated control

CLD number: TP273

Document code: A

Article ID: 1674-8042(2018)03-0269-10

doi: 10.3969/j.issn.1674-8042.2018.03.009

0 Introduction

At present, due to operation constraint of “power determined by heat” of cogeneration units, the peak-shaving capacity of power system is insufficient in heating period. Therefore, main contradiction in the development of wind power is still caused by wind power curtailment^[1-2]. Besides, wind power output is volatile, intermittent and uncertain. If it is paralleled in power grid, there exists a great challenge to its stable operation and difficulty of wind power integration accommodation^[3-4].

In order to decouple operation constraint of “power determined by heat” of cogeneration units, stabilize wind power output fluctuations, and improve networking scale of wind power, energy storage technology has been widely concerned at home and abroad because of its good wind power complementarity^[5-7]. Recently, in addition to pumped storage which has been mature, other energy storage methods are faced with problems whose scale, cost, life and efficiency cannot meet the requirements of modern power system. As for wind

power accommodation, in Ref. [8], configuration theory was used to expand wind in power operation feasible domain by output distribution between wind power and pumped storage. In Ref. [9], wind power acceptance capacity and system economy were studied in case of different wind power permeabilities and different storage capacity scenarios. Through configuration of thermal energy storage and electrical boiler in cogeneration plants, the thermoelectric coupling relationship is broken^[10-11]. As for wind power stabilization, in Ref. [12], power was distributed between super capacitors and batteries to stabilize wind power fluctuations at different time scales. In Ref. [13], electric vehicles and interruptible load were directly controlled to reduce the burden of power grid operation. In Ref. [14], the first-order low-pass filter was used as a wind power stabilization method. However, most of the current studies separately consider the problems of wind power accommodation and its fluctuation stabilization, to a certain extent, which leads to the difficulty of coordination management.

In view of difficulty of wind power accommodation

and stabilization of wind power fluctuations, a two-level coordinated control strategy based on electric heat storage and pumped storage is proposed in this paper. The optimal control is carried out according to plan of previous day and real-time situation at different time scales, which can not only improve wind power accommodation, but also reduce the impact of wind power fluctuations on frequency adjustment units.

1 Thermoelectric load and wind power output characteristics

1.1 Characteristics of thermoelectric load and wind power output distribution during heating period

By analysis of previous data, the distribution of electric load is opposite to thermal load, and wind power output characteristics and thermal load trends are roughly the same. In the night of wind power season, the situation of wind power curtailment is most serious in this period, as shown in Fig. 1. If wind power can be converted into heat and then stored, the heat will be used as the peaking source of thermal network at night, which can not only improve peak-shaving capacity of hot grid, but also decouple thermoelectric coupling of cogeneration units, so as to improve peak-shaving capacity of power system and allocate more networking space to wind power. Since only peak-shaving of electric heat storage can not completely consume wind power, large-scale wind power integration is detrimental to power system stability. If pumped storage and electric heat storage operate together, the wind power curtailment and its fluctuations can be further eliminated.

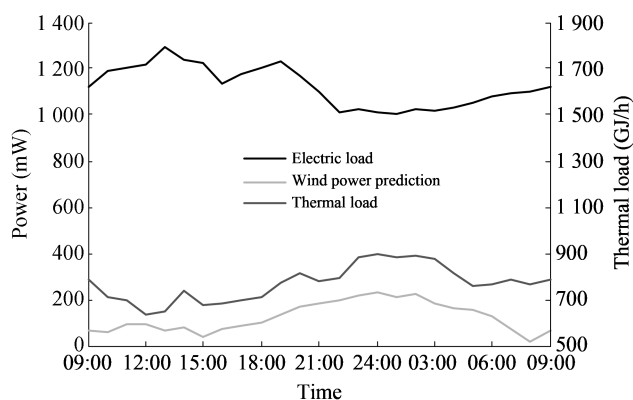


Fig. 1 Thermoelectric load and wind power distribution during heating period

1.2 Characteristics of wind power real-time fluctuation

The real-time output process of wind power is generally described by fluctuation characteristics of time scale in minute. The output fluctuation curve of a wind farm is shown in Fig. 2.

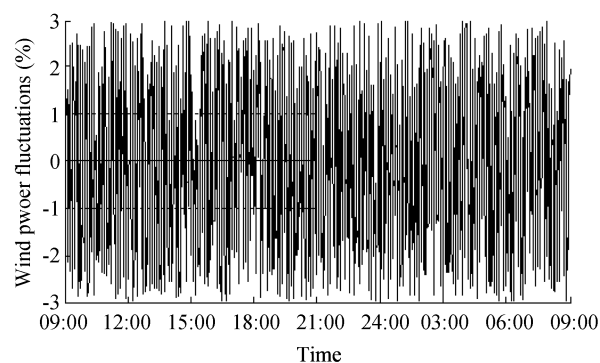


Fig. 2 Real-time fluctuation curve of wind power output

According to fluctuation range, the fluctuations are divided into two cases: small fluctuations are in $[-1\%, 1\%]$, and large fluctuations are outside $[-1\%, 1\%]$. In $[-1\%, 1\%]$, wind power outputs are relatively stable, and the fluctuations are small; outside $[-1\%, 1\%]$, the fluctuations are large, will cause a larger prediction error.

2 Combined system structure with electric heat storage

The structure of the combined system with electric heat storage is shown in Fig. 3.

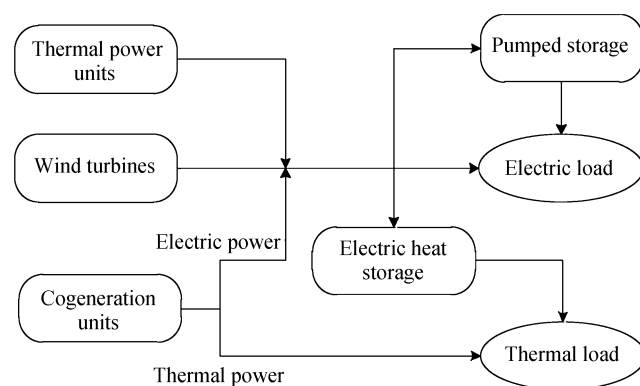


Fig. 3 Structure diagram of combined system

Electric heat storage has advantages of large capacity and high efficiency, which can supply cogeneration units with heat together to reduce the effect of “power determined by heat” operation constraint of cogeneration units on peak-shaving

capacity in heating period. Besides, if electric heat storage participates in heating, the electrical load of the system will be increased, thus expanding wind power accommodation space.

3 Coordinated control strategy based on electric heat storage and pumped storage

3.1 Coordinated control strategy

Based on the above-mentioned analysis of wind power fluctuation characteristics and the capacity of wind power accommodation of the combined system with electric heat storage, a two-level coordinated control strategy based on electric heat storage and pumped storage is proposed to promote wind power accommodation and stabilize its fluctuations. The process is shown in Fig. 4.

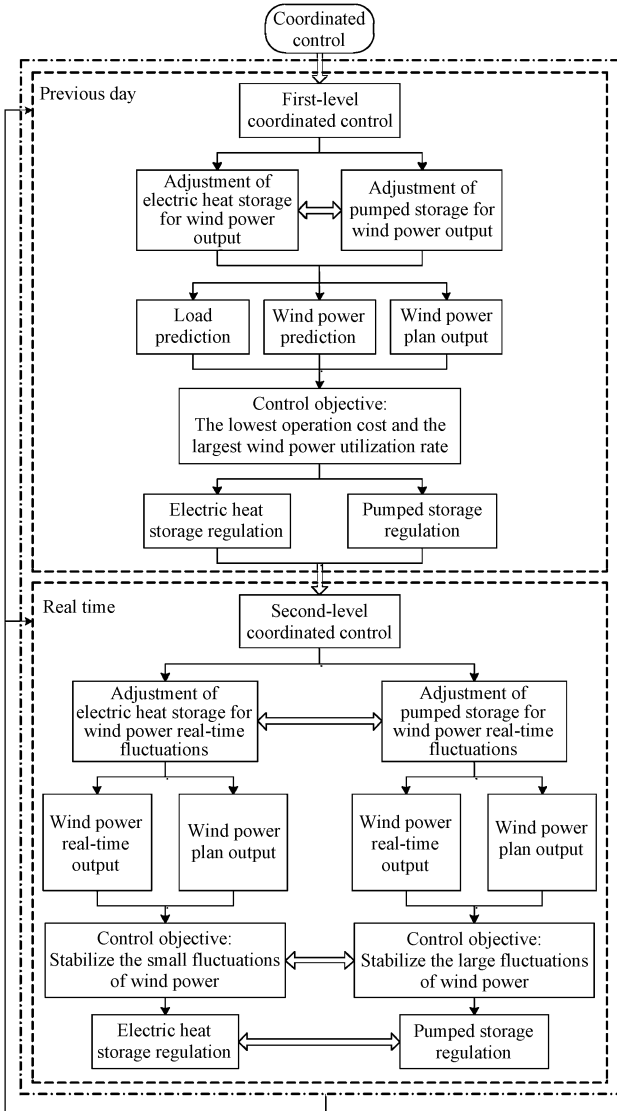


Fig. 4 Block diagram of coordinated control strategy

For the coordinated control of electric heat storage and pumped storage, the first-level coordinated control belongs to planning dispatch control. It mainly promotes wind power accommodation and operation economy, and the adjustment time scale is longer. By means of coordinated operation of electric heat storage and pumped storage at different time intervals, wind power curtailment generated by restrictions of the capacity of conventional units can be eliminated as much as possible. The second-level coordinated control is a real-time tracking control. It requires faster regulation, therefore it needs complementary adjustment capacity of electric heat storage and pumped storage to respond and regulate real-time fluctuations of wind power.

3.2 First-level coordinated control

Considering priority of wind power integration, the optimal scheduling model does not take account of cost of wind power generation. Cogeneration units need to heat the system, so it cannot stop working. The electric and thermal output of cogeneration units are converted into the output under pure cogeneration conditions. The optimization objectives of the first-level coordinated control are built considering wind power utilization and system operation economy, respectively.

1) Objective function 1: The operation cost of the system is the lowest, namely

$$\min F_1 = \sum_{t=1}^{N_T} \left\{ \sum_{i=1}^{N_R} U_{i,t} [f_1(P_{H,i,t}) + (1 - U_{i,t-1})S_i + C_{ri}(R_{i,t}^u, R_{i,t}^d)] + \sum_{j=1}^{N_G} f_2(P_{E,j,t}, P_{C,j,t}) + \sum_{k=1}^{N_H} (S_{k,t}^{\text{gen}} + S_{k,t}^{\text{pum}}) \right\}, \quad (1)$$

where $U_{i,t}$ is the start-stop state of thermal power unit i in time interval t ; $P_{H,i,t}$ and $f_1(P_{H,i,t})$ are the output power and the power generation costs of thermal power unit i in time interval t , respectively; S_i and $C_{ri}(R_{i,t}^u, R_{i,t}^d)$ are the starting costs and reserving costs of thermal power unit i , respectively; $R_{i,t}^u$ and $R_{i,t}^d$ are the positive and negative spinning reserve capacity of thermal power unit i in time interval t , respectively; $P_{E,j,t}$, $P_{C,j,t}$ and $f_2(P_{E,j,t}, P_{C,j,t})$ are the electric output, heat output and operating costs of cogeneration unit j in time interval t , respectively; $S_{k,t}^{\text{gen}}$ and $S_{k,t}^{\text{pum}}$ are the start-up costs under the power generation condition and pumping condition of pumped storage unit k in time

interval t , respectively; N_T is the number of time periods for a scheduling cycle; and N_R , N_G and N_H are the total number of thermal power units, cogeneration units and pumped storage units, respectively.

The operating cost equation of thermal power units is

$$f_1(P_{H,i,t}) = a_i P_{H,i,t}^2 + b_i P_{H,i,t} + c_i, \quad (2)$$

where a_i , b_i and c_i are the operating cost coefficients of thermal power units.

The operating cost equation of cogeneration units is

$$f_2(P_{E,j,t}, P_{C,j,t}) = a_j (P_{E,j,t} + C_v P_{C,j,t})^2 + b_j (P_{E,j,t} + C_v P_{C,j,t}) + c_j, \quad (3)$$

where a_j , b_j and c_j are operating cost coefficients of cogeneration units, and C_v is conversion coefficient of pure condensate state of cogeneration units.

The equation of reserving cost is

$$C_{ri}(R_{i,t}^u, R_{i,t}^d) = k_{i,t}^u R_{i,t}^u + k_{i,t}^d R_{i,t}^d, \quad (4)$$

where $k_{i,t}^u$ and $k_{i,t}^d$ are the positive and negative reserving costs, respectively.

The equations of starting costs of pumped storage unit under different operation states are

$$\begin{cases} S_{k,t}^{\text{gen}} = S_k^{\text{gen}} I_{k,t}^{\text{gen}} (I_{k,t}^{\text{gen}} - I_{k,t-1}^{\text{gen}}), \\ S_{k,t}^{\text{pum}} = S_k^{\text{pum}} I_{k,t}^{\text{pum}} (I_{k,t}^{\text{pum}} - I_{k,t-1}^{\text{pum}}), \end{cases} \quad (5)$$

where S_k^{gen} and S_k^{pum} are the starting costs under the power generation condition and pumping condition of pumped storage unit k , respectively; $I_{k,t}^{\text{gen}}=1$ and $I_{k,t}^{\text{pum}}=1$ mean that pumped storage unit is in the power generation condition and pumping condition in time interval t , respectively.

2) Objective function 2: The wind power curtailment is the least, namely

$$\min F_2 = \sum_{t=1}^{N_T} (P_{f,t}^{\text{wind}} - P_{\text{plan},t}^{\text{wind}}), \quad (6)$$

where $P_{f,t}^{\text{wind}}$ and $P_{\text{plan},t}^{\text{wind}}$ are wind power forecast and planning dispatch output, respectively.

The constraints are as follows.

① The power balance constraint is

$$\sum_{i=1}^{N_R} P_{H,i,t} + \sum_{j=1}^{N_G} P_{E,j,t} + \sum_{k=1}^{N_H} P_{\text{PS},k,t} + P_{\text{wf},t} = P_{\text{load},t} + P_{\text{ES},t}, \quad (7)$$

where $P_{\text{PS},k,t}$ is the output of pumped storage k in

time interval t ; plus and minus represent the power generation state and pumping state, respectively; $P_{\text{wf},t}$ and $P_{\text{ES},t}$ are the wind farm output and consumed electric power of electric heat storage in time interval t , respectively.

② The heat balance constraint is

$$\sum_{j=1}^{N_G} P_{C,j,t} = P_{\text{load},t}^{\text{th}} - P_{\text{ES},t}^{\text{th}}, \quad (8)$$

where $P_{\text{load},t}^{\text{th}}$ and $P_{\text{ES},t}^{\text{th}}$ are the heat load of the system and heating power of electric heat storage in time interval t , respectively.

③ The unit output constraint is

$$U_{i,t} P_{i,\min} \leq P_{i,t} \leq U_{i,t} P_{i,\max}, \quad (9)$$

where $P_{i,\max}$ and $P_{i,\min}$ are the upper and lower limits of unit t , respectively.

④ The unit climbing constraint is

$$|P_{i,t} - P_{i,t-1}| \leq I_i^{\text{ramp}}, \quad (10)$$

where I_i^{ramp} is the rise and fall speed of unit i .

⑤ The pumped storage capacity constraint is

$$\frac{V_0 - V_{\max}}{\eta^{\text{pum}}} \leq \frac{\sum_{t=1}^{\tau} P_{\text{PS},t}^{\text{gen}} \eta^{\text{gen}}}{\eta^{\text{pum}}} - \sum_{t=1}^{\tau} P_{\text{PS},t}^{\text{pum}} \leq \frac{V_0 - V_{\min}}{\eta^{\text{pum}}}, \quad (11)$$

where η^{pum} and η^{gen} are the water-electricity conversion coefficients for pumping and power generation of pumped storage; V_0 is the initial water volume of the upper reservoir; V_{\max} and V_{\min} are the maximum and minimum water volume of the upper and lower reservoirs, respectively.

The above formula represents the upper reservoir capacity constraint of pumped storage. Because the total storage capacity of the upper and lower reservoirs is constant during pumping and power generation process, the capacity constraint of the lower reservoir is also considered.

⑥ The minimum starting and stopping time constraints are

$$\begin{cases} (U_{i,t-1} - U_{i,t})(T_{i,t}^{\text{on}} - T_{i,\min}^{\text{on}}) \geq 0, \\ (U_{i,t} - U_{i,t-1})(T_{i,t}^{\text{off}} - T_{i,\min}^{\text{off}}) \geq 0, \end{cases} \quad (12)$$

where $T_{i,t}^{\text{on}}$ and $T_{i,t}^{\text{off}}$ are the continuous running time and continuous down time of unit i in time interval t , respectively; $T_{i,\min}^{\text{on}}$ and $T_{i,\min}^{\text{off}}$ are the minimum continuous running time and the minimum continuous down time of unit i , respectively.

⑦ The spinning reserve constraint is

$$\begin{cases} R_{i,t}^u \leq \min(U_{i,t}P_{i,\max} - U_{i,t}P_{i,t}, U_{i,t}P_i^{\text{ramp}}), \\ R_{i,t}^d \leq \min(U_{i,t}P_{i,t} - U_{i,t}P_{i,\min}, U_{i,t}P_i^{\text{ramp}}). \end{cases} \quad (13)$$

The planning dispatch output of wind power $P_{W_{\text{plan},t}}$ generated by the first-level coordinated control is the maximum wind power accommodation within the regulation capacity of electric heat storage and pumped storage. It is passed to the second-level coordinated control as reference value.

$$P_{W_{\text{plan},t}} = P_{\text{plan},t}^{\text{wind}} + \Delta P_{\text{ES},t} + \Delta P_{\text{PS},t}, \quad (14)$$

where $\Delta P_{\text{ES},t}$ and $\Delta P_{\text{PS},t}$ are the wind power accommodation quota of electric heat storage and pumped storage in time interval t , respectively.

3.3 Second-level coordinated control

The second-level coordinated control based on the first-level coordinated control is to eliminate fluctuations between real-time output and planning output of wind power by regulating working state

and output of electric heat storage and pumped storage.

According to the planning output of wind power obtained by Eq. (14), the real-time output fluctuations of wind power can be calculated by

$$P_W = |P_{\text{real}}^{\text{wind}} - P_{W_{\text{plan}}}|. \quad (15)$$

According to the real-time fluctuations of wind power output, the power fluctuations are divided into small fluctuations and large fluctuations. The output power which fluctuates within $\pm 1\%$ of the planning output (within the dotted line in Fig. 2) has a small fluctuation, and the output power which fluctuates out of $\pm 1\%$ of the planning output (outside the dotted line in Fig. 2) has a large fluctuation. For small fluctuations and large fluctuations, the second-level coordinated control method are shown in Table 1, where $P_{W,\max}$ and $\Delta P_{\max}^{\text{PS}}$ are the limit of wind power fluctuations and the limit of adjustment capacity of pumped storage, respectively.

Table 1 Second-level coordinated control strategy

P_W	Control method	Control objective
$< P_{W,\max}$	Electric heat storage regulation	Stabilize small fluctuations
$[P_{W,\max}, \Delta P_{\max}^{\text{PS}}]$	Pumped storage regulation	Stabilize large fluctuations
$> \Delta P_{\max}^{\text{PS}}$	Wind power curtailment regulation	Quasi regulation

The regulation amount is calculated as follows.

1) The fluctuation P_W of wind power are determined based on the comparison of planning output and real-time output of wind farms.

2) According to the electrical split information of local source path, the distribution factor $d_{W1} = P_{\text{wf-ES}}/P_{\text{wf}}$ which is sent to electric heat storage by wind farm output power P_{wf} and the distribution factor $d_{W2} = P_{\text{wf-PS}}/P_{\text{wf}}$ which is sent to pumped storage by wind farm output power are determined, and the absorption factor $d_{F1} = P_{\text{wf-ES}}/P_{\text{ES}}$ which is absorbed from wind farms by electric heat storage power P_{ES} and the absorption factor $d_{F2} = P_{\text{wf-PS}}/P_{\text{PS}}$ which is absorbed from wind farms by pumped storage power P_{PS} are determined, where $P_{\text{wf-ES}}$ is the sum of transmission power on all split paths between wind farms and electric heat storage, and $P_{\text{wf-PS}}$ is the sum of transmission power on all split paths between wind farms and pumped storage^[15].

3) According to wind power output fluctuations in each time period, the regulation amount of electric heat storage and pumped storage for wind farm

output fluctuations is calculated by

$$\Delta P_{\text{ES}}^{\text{wind}} = d_{W1}d_{F1}P_W = \frac{P_{\text{wf-ES}}^2}{P_{\text{wf}}P_{\text{ES}}} |P_{\text{real}}^{\text{wind}} - P_{W_{\text{plan}}}|, \quad (16)$$

$$\Delta P_{\text{PS}}^{\text{wind}} = d_{W2}d_{F2}P_W = \frac{P_{\text{wf-PS}}^2}{P_{\text{wf}}P_{\text{PS}}} |P_{\text{real}}^{\text{wind}} - P_{W_{\text{plan}}}|. \quad (17)$$

4 Solving method

In this paper, a complex multi-objective and multi-period optimization method is proposed, which has characteristics of high dimension, multiple constraints and nonlinearity. The traditional optimization algorithm is difficult to solve this complicated optimization problem, therefore a harmony search algorithm (multi-objective harmony search, MOHS) is adopted, which has a strong search ability and fast convergence speed to solve the optimization model^[16-17]. Moreover, the weighted scale method is used to make multi-objective decision. Assuming that the system operator has the same preference for different objects, the weight

coefficient is $K = [0.5, 0.5]$. The implementation process is as follows.

1) The parameters is initialized. The algorithm parameters to be initialized include harmony memory search (HMS), harmony memory considering rate (HMCR) and the number of final iterations G_{\max} .

2) The dominant relationship is determined. The multi-objective optimization is defined as

$$\min\{F_1(X), F_2(X), \dots, F_m(X)\}, X \in V, \quad (18)$$

where the decision variable $X = (x_1, x_2, \dots, x_n)^V$ is within the range of V . In general, each object is mutually exclusive, so it is necessary to determine the dominant relationship between the various harmonies. If the decision variables X_1 and X_2 satisfy Eq.(19), it can be determined that the decision variable X_2 is dominated by the other decision variable X_1 , namely

$$\begin{cases} \forall i : f_i(X_1) \leq f_i(X_2), \\ \exists i \mid f_i(X_1) < f_i(X_2), \end{cases} \quad i = 1, \dots, m. \quad (19)$$

3) The crowding degrees of the same level harmonies are calculated. Besides, they are sorted according to the crowding degrees.

4) The hybrid strategy is used to produce new harmonies. As the number of iterations increases, the diversity of the solution in the algorithm will decrease, but increasing the diversity of the solution will lead to the decrease of the convergence rate. Therefore, this paper uses hybrid strategy to produce new harmonies. The new harmonies generation algorithm is

$$X^{\text{new}} = X^{\text{Nd}} \pm \text{rand} \mid X^{\text{Nd}} - X^{\text{d}} \mid, \quad (20)$$

where X^{new} is the new harmony produced; X^{Nd} and X^{d} are the randomly selected non-dominated and dominated harmonies, respectively; and rand is the random number which is generated by the HMCR algorithm.

5) The harmony memory (HM) is updated. The harmony whose solution is the worst after initialization is replaced by the new harmony.

6) Determine whether the algorithm reaches the termination condition. If not, return to step 4 to cycle until the number of iterations is G_{\max} , or else the algorithm ends.

5 Simulation

5.1 Basic data

In order to verify the feasibility and effectiveness of the coordinated control strategy based on electric heat storage and pumped storage, taking the wind farm of Jiuquan new energy base in Gansu as an example, the simulation was carried out. The installed capacity of the wind farm is 300 MW, and its prediction is shown in Table 2. The prediction of electric load and thermal load is shown in Table 3. The parameters of pumped storage unit are shown in Table 4. The parameters of thermal power unit are shown in Table 5. The parameters of cogeneration unit are shown in Table 6. The dispatch cycle is 1 d, and 1 h is a dispatch period.

Table 2 Wind power prediction

Time	Prediction (MW)	Time	Prediction (MW)	Time	Prediction (MW)	Time	Prediction (MW)
06:00	130.05	12:00	95.48	18:00	101.32	24:00	232.46
07:00	77.01	13:00	67.64	19:00	134.48	01:00	212.16
08:00	17.18	14:00	78.01	20:00	169.29	02:00	224.35
09:00	67.55	15:00	40.25	21:00	183.45	03:00	182.83
10:00	57.83	16:00	73.01	22:00	197.04	04:00	167.46
11:00	97.02	17:00	87.26	23:00	216.17	05:00	156.25

Table 3 Prediction of electric load and thermal load

Time	P_{load} (MW)	$P_{\text{load}}^{\text{th}}$ (GJ/h)	Time	P_{load} (MW)	$P_{\text{load}}^{\text{th}}$ (GJ/h)	Time	P_{load} (MW)	$P_{\text{load}}^{\text{th}}$ (GJ/h)
06:00	1 077.19	767.58	14:00	1 237.54	736.44	22:00	1 014.79	795.20
07:00	1 089.76	783.47	15:00	1 226.15	675.91	23:00	1 023.62	881.18
08:00	1 099.61	766.16	16:00	1 135.93	683.25	24:00	1 012.23	899.53
09:00	1 124.38	787.93	17:00	1 172.08	694.81	01:00	1 005.32	884.26
10:00	1 188.02	712.55	18:00	1 204.92	709.73	02:00	1 022.45	892.75
11:00	1 205.25	694.32	19:00	1 228.55	774.56	03:00	1 017.63	875.08
12:00	1 216.41	631.24	20:00	1 167.62	817.42	04:00	1 031.22	818.36
13:00	1 291.33	648.39	21:00	1 103.41	782.12	05:00	1 053.38	759.24

Table 4 Operating parameters of pumped storage unit

Unit	Upper reservoir ($\times 10^3 \text{ m}^3$)				Lower reservoir ($\times 10^3 \text{ m}^3$)			S^{gen} (\$)	S^{pum} (\$)	$P_{\text{max}}^{\text{gen}}$ (MW)	P^{pum} (MW)
	V_{max}	V_{min}	V_0	V_{end}	V_{max}	V_{min}	V_0				
PU-1	15	5	10	10	45	35	40	250	400	60	40.1
PU-2	15	5	10	10	45	35	40	250	400	60	40.1

Table 5 Operating parameters of thermal power unit

Unit	P_{min} (MW)	P_{max} (MW)	P^{ramp} (MW/h)	$T_{\text{min}}^{\text{on}}$ (h)	$T_{\text{min}}^{\text{off}}$ (h)	a (\$/h)	b (\$/MW)	c (\$/MW ²)	S (\$)
G1	400	150	200	8	8	0.000 48	16.19	1 000	5 960
G2	400	150	200	8	8	0.000 31	17.26	970	5 960
G3	130	60	100	6	6	0.002 20	16.61	700	2 620

Table 6 Operating parameters of cogeneration unit

Unit	P_{min} (MW)	P_{max} (MW)	P_{Cmax} (MW)	P^{ramp} (MW/h)	a (\$/h)	b (\$/MW)	c (\$/MW ²)	C_v
G4	150	70	200	50	0.000 68	32	450	0.15
G5	150	70	200	50	0.000 68	32	450	0.15

5.2 Result analysis

The case includes three systems as follows.

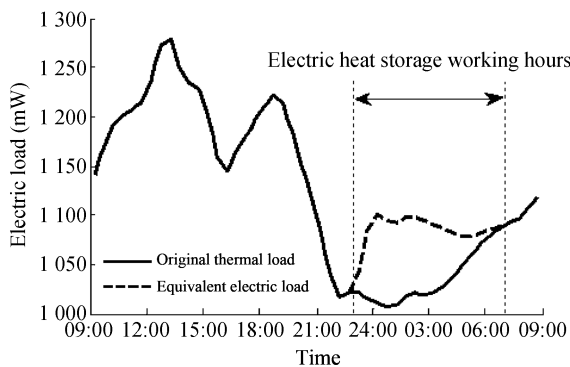
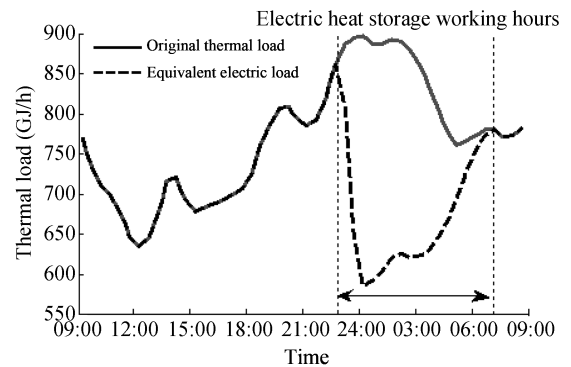
System I: It does not contain electric heat storage and pumped storage. Conventional cogeneration plants supply heat to thermal load, and conventional power supplies supply power to electric load.

System II: It contains electric heat storage. Electric heat storage and cogeneration units collaboratively supply heat to thermal load, and conventional power supplies supply power to electric

load.

System III: It contains electric heat storage and pumped storage. Electric heat storage and cogeneration units collaboratively supply heat to thermal load, and conventional power supplies and pumped storage collaboratively supply power to electric load.

The contrast curves of equivalent electric load and equivalent heat load before and after the configuration of electric heat storage are shown in Figs. 5 and 6, respectively.

**Fig. 5 Contrast curves of equivalent electric load****Fig. 6 Contrast curves of equivalent thermal load**

It can be seen from the contrast curves of equivalent electric load and equivalent heat load before and after the operation of electric heat storage, when electric heat storage is involved in heating, the equivalent electric load is increased significantly, and the equivalent thermal load is significantly reduced during the peak period of thermal load. It indicates that not only the peak of thermal load can be adjusted by electrothermal conversion after electric heat storage operation, but also the electric load of the system is increased, which therefore plays the role of cutting thermal load

peak and filling electric load valley.

Wind power planning dispatch output curves of different systems are shown in Fig. 7.

It can be seen from Fig. 7, in case that electric heat storage and pumped storage are not equipped in the system, the wind power curtailment is very serious from 21:00 of the previous day to 8:00 of the next day. When electric heat storage is equipped in the system and collaboratively heats with cogeneration plants, the effect of eliminating wind power curtailment is very obvious in the heat load peak period (23:00 – 07:00), but the situation of wind

power curtailment is not improved in the non-operating period of electric heat storage. When electric heat storage and pumped storage are equipped in the system and work together, the wind power is consumed to the maximum extent.

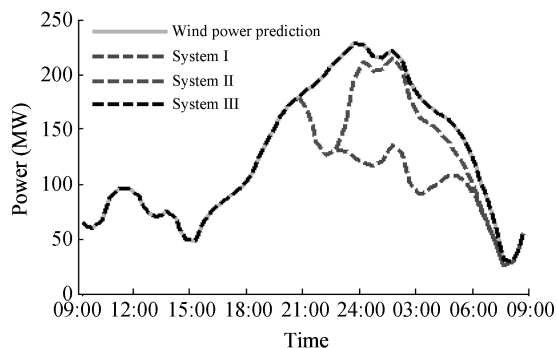


Fig. 7 Contrast curves of wind power scheduling output

According to the above analysis, the system performs at the lowest cost and the maximum utilization of wind power. When electric heat storage and pumped storage work together. The respective adjustments are shown in Fig. 8.

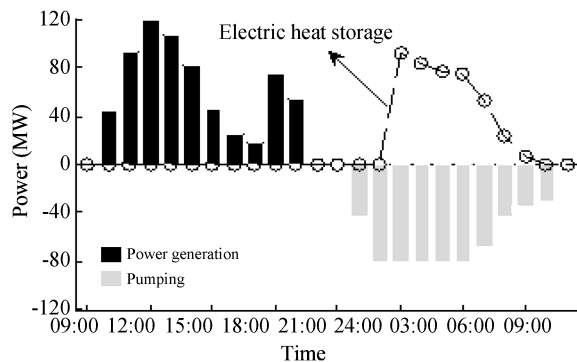


Fig. 8 Electric heat storage and pumped storage regulation

It can be seen from electric heat storage adjustment curve, electric heat storage begins to peak and store heat in electric load valley period (23:00–07:00). In other periods, electric heat storage is closed and its heat storage system heats the users.

When the wind power is still obstructed in the system, pumped storage starts to pump (pump mode); when the net load of the system is more than 0 but less than the start power of pumped storage units, pumped storage is at rest; when the net load of the system is more than the starting power of pumped storage units, pumped storage begins to generate electricity (turbine mode).

The scheduling results before and after the coordinated operation of electric heat storage and pumped storage are shown in Table 7.

Table 7 Comparison of dispatch results of three systems

System	Wind power curtailment (MW · h)	Wind power utilization rate (%)	Total cost (\$)
System I	705.75	76.98	814 670.26
System II	291.17	90.50	767 096.78
System III	0	100	736 043.91

It can be seen that if electric heat storage is equipped in the system, conventional cogeneration plants and electric heat storage co-heating can not only greatly eliminate wind power curtailment to improve the wind power accommodation rate, but also help to reduce the total scheduling cost to improve operation economy of the system. However, because part of wind power is still blocked when electric heat storage is equipped in the system, the coordinated operation of electric heat storage and pumped storage can further promote wind power accommodation and help to improve operation economy of the system.

The second-level coordinated control of electric heat storage and pumped storage was carried out taking 30 min as a operation cycle, and the real-time fluctuations of wind power are stabilized with a time scale of 1 min to ensure the safety and reliability of the system. The real-time fluctuation curve of wind power output is shown in Fig. 9. The maximum fluctuation is 2.88%, and the stabilization target is 183.45 MW.

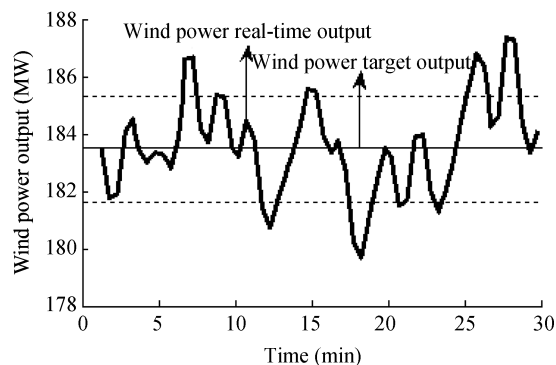


Fig. 9 Real-time fluctuations of wind power output before the second-level coordinated control

The stabilization effect of wind power output fluctuations generated by the second-level coordinated control of electric heat storage and pumped storage is shown in Fig. 10. The wind power real-time output which fluctuates within $\pm 1\%$ of planning output is small fluctuation, therefore, electric heat storage adjusts; the wind power real-time output which fluctuates outside $\pm 1\%$ of planning output is large fluctuation, therefore,

pumped storage adjusts. After the second-level coordinated control, wind power is stable at around 183.45 MW with the maximum fluctuation of 0.58%, meeting the safety and reliability requirements of wind power integration.

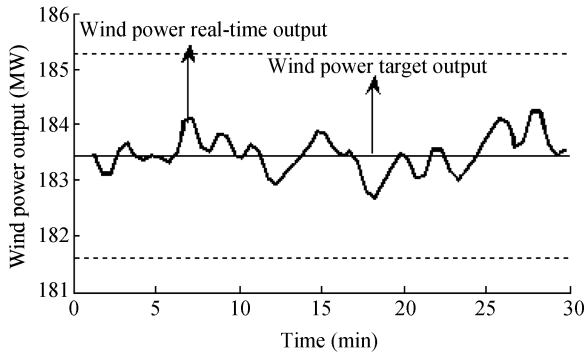


Fig. 10 Real-time fluctuations of wind power output after the second-level coordinated control

6 Conclusions

1) Through the first-level coordinated operation of electric heat storage and pumped storage, the operation constraint of “power determined by heat” of cogeneration units can be decoupled by electrothermal conversion, and the blocked wind power can be consumed. The rate of wind power curtailment is decreased by 23.02% compared with the system without electric heat storage and pumped storage, and decreased by 9.50% compared with the system only with electric heat storage without pumped storage.

2) The operation cost of the system with the coordinated operation of electric heat storage and pumped storage is the lowest, which is reduced by 9.65% compared with the system without electric heat storage and pumped storage, and reduced by 4.05% compared with the system only with electric heat storage.

3) The maximum real-time fluctuation of wind power is decreased from 2.88% to 0.58% by means of the second-level coordinated operation of electric heat storage and pumped storage. The grid wind power is basically stable around the planning dispatch output.

Therefore, the coordinated control strategy based on electric heat storage and pumped storage proposed in this paper can further expand wind power accommodation space, stabilize fluctuations of wind power, save the operation cost of the system and provide a new control means and theoretical method

for wind power integration.

References

- [1] Wang Z B. Wind power abandoned rationing report of China. *Energy*, 2014; 42-48.
- [2] Mu G, Cui Y, Liu J, et al. Source-grid coordinated dispatch method for transmission constrained grid with surplus wind generators. *Automation of Electric Power Systems*, 2013, 37(6): 24-29
- [3] Wang X H, Qiao Y, Lu Z X, et al. A novel method to assess wind energy usage in the heat-supplied season. *Proceedings of the CSEE*, 2015, 35(9): 2112-2119.
- [4] Gu Z P, Kang C Q, Chen X Y, et al. Operation optimization of integrated power and heat energy systems and the benefit on wind power accommodation considering heating network constraints. *Proceedings of the CSEE*, 2015, 35(14): 3596-3604.
- [5] Yuan X M, Cheng S J, Wen J Y. Prospects analysis of energy storage application in grid integration of large-scale wind power. *Automation of Electric Power Systems*, 2013, 37(1): 14-18.
- [6] Liu D Y, Tan Z Z, Wang F. Study on combined system with wind power and pumped storage power. *Water Resources and Power*, 2006, 24(6): 39-42.
- [7] Yan G G, Liu J, Cui Y, et al. Economic evaluation on improving wind power scheduling scale by using energy storage systems. *Proceedings of the CSEE*, 2013, 33(22): 45-52.
- [8] Hu Z C, Ding H J, Kong T. A joint daily operational optimization model for wind power and pumped-storage plant. *Automation of Electric Power Systems*, 2012, 36(2): 36-41.
- [9] Li F, Zhang L Z, Shu J, et al. A study on peak load regulation and economic leaning of wind power and energy storage system. *East China Electric Power*, 2012, 40(10): 1696-1700.
- [10] Lyu Q, Chen T Y, Wang H X, et al. Combined heat and power dispatch model for power system with heat accumulator. *Electric Power Automation Equipment*, 2014, 34(5): 79-85.
- [11] Lyu Q, Jiang H, Chen T Y, et al. Wind power accommodation by combined heat and power plant with electric boiler and its national economic evaluation. *Automation of Electric Power Systems*, 2014, 38(1): 6-12.
- [12] Jiang Q Y, Hong H S. Wavelet-based capacity Configuration and coordinated control of hybrid energy storage system for smoothing out wind power fluctuations. *IEEE Transactions on Power Systems*, 2013, 28(2): 1363-1372.
- [13] Ai X, Liu X. Chance constrained model for wind power usage based on demand response. *Journal of North China Electric Power University (Natural Science Edition)*, 2011, 38(3): 17-35.
- [14] Guo J J, Wu H B. Hybrid energy storage coordinated optimal control method for stabilizing wind power fluctua-

tion. *Acta Energiæ Solaris Sinica*, 2016, 37(10): 2695-2702.

- [15] Chen N, Yu J L. Active power dispatch and regulation of wind power system based on electrical dissecting information of electric power network. *Proceedings of the CSEE*, 2008, 28(16): 51-58.

[16] Geem Z W, Kim J H, Loganathan G V. A new heuristic optimization algorithm: harmony search. *Simulation*, 2011, 76(2): 60-68.

[17] Zou D X, Gao L Q, Wu J H, et al. A novel global harmony search algorithm for reliability problems. *Computers & Industrial Engineering*, 2010, 58(2): 307-316.

基于电蓄热与抽水蓄能的风电消纳协调控制策略

李守东¹, 董海鹰¹, 张蕊萍¹, 马喜平²

(1. 兰州交通大学 自动化与电气工程学院, 甘肃 兰州 730070;

2. 国网甘肃省电力公司 电力科学研究院, 甘肃 兰州 730050)

摘要: 为解决“三北”地区冬季供热期由于热发电机组“以热定电”运行约束而导致的严重弃风问题, 该文在研究电热负荷与风电出力分布特性以及不同时间尺度风功率波动特性的基础上, 提出了基于电蓄热与抽水蓄能的两级协调控制策略。第一级协调控制以系统运行成本最小和风电利用率最大为目标, 根据电热负荷和风电预测出力, 通过电蓄热与抽水蓄能在调节容量上的优化配置, 提高系统运行经济性和风电消纳率; 第二级协调控制针对风电出力的实时波动, 根据风电计划上网偏差, 通过电蓄热与抽水蓄能的协调控制, 平抑风电实时波动, 提高风电消纳水平。结合甘肃酒泉实际运行的风电场站, 所提出的协调控制策略的有效性得到验证。

关键词: 风电消纳; 电蓄热; 抽水蓄能; 风电波动; 协调控制

引用格式: LI Shou-dong, DONG Hai-ying, ZHANG Rui-ping, et al. Coordinated control strategy for wind power accommodation based on electric heat storage and pumped storage. *Journal of Measurement Science and Instrumentation*, 2018, 9(3): 269-278. [doi:10.3969/j.issn.1674-8042.2018.03.009]